Anonymous Referee #2

General remarks

This manuscript investigates how the revised representation of soil organic matter, together with a mineral compaction adjustment, influences land surface processes within the ISBA-CTRIP modeling system. The study addresses an important and often overlooked inconsistency in compaction status between pedotransfer-function-based soil properties and bulk density estimates derived from SoilGrids, and proposes a more physically consistent framework to account for compaction effects. Overall, the manuscript makes a valuable contribution by quantifying the impact of these processes on global land simulations.

Response: We thank the reviewer for this positive assessment of the manuscript and for recognizing the contribution of the proposed framework to the representation of soil organic matter and mineral soil compactness effects in land surface modeling.

Major comments

Remark 1: The manuscript discusses the analytical formulation used to diagnose organic matter bulk density (ρ_{bom}), noting that the function may become numerically unstable when ρ_b approaches ρ_{bms}, potentially leading to divergence or nonphysical values. To mitigate this issue, a lower bound is applied to f_{mom} in the computation of ρ_{bom}. However, the implementation in Part 1 (Decharme, 2025) uses the uncorrected f_{mom}, which introduces an inconsistency between the theoretical formulation and its numerical application. The relatively large values of DE25c compared to DE25 in Figure 3 suggest that this bound does indeed exert a strong influence. It would be helpful if the authors could provide a spatial diagnostic showing where the lower bound is active (i.e., grid cells where f_{mom} is constrained), in order to better assess the robustness of this bound. In addition, a brief sensitivity analysis of key results using the corrected f_{mom} would help evaluate how much the prescribed lower bound affects the main conclusions, and whether this numerical treatment could alter any of the conclusions presented in Part 1.

Response: We agree that the numerical treatment used in the diagnostic computation of ρ_{bom} needed to be documented more explicitly. The lower bound applied to f_{mom} is not intended to represent a physical change in SOM content. It is a numerical safeguard used only in the computation of ρ_{bom} when Equation 2 becomes ill-conditioned, which occurs when f_{mom} is very small and ρ_b approaches the mineral-phase bulk density. In this limit, the organic contribution to the bulk soil properties is expected to remain small, but the analytical expression for ρ_{bom} can diverge or produce nonphysical values. We therefore clarified in Sect. 2.2.2 that f_{mom}^* is the regularized value of f_{mom}, introduced as a numerical safeguard in the diagnostic computation of ρ_{bom}. We also revised Sect. 3.1.3 to quantify where this safeguard is activated and to show that it remains confined to low-SOC, mineral-dominated conditions. To document this point, we added hatching in the ρ_{bom} panels of Supplementary Figure S4 and in the corresponding f_{vom} panels of Supplementary Figure S5. In DE25, the safeguard is activated over 0.97, 1.88, 9.98, 14.04, and 15.67% of valid land grid points at 0.5, 7, 50, 90, and 175 cm depth, respectively. In DE25c, the corresponding fractions are 0, 0, 0.12, 1.11, and 1.59%. These fractions show that the compactness-adjusted formulation strongly reduces the occurrence of this numerical safeguard. We further characterized the affected grid points. In DE25, they are mainly located in desert areas and other low-SOC regions. Their median f_{moc} decreases from 0.0103 kg kg^{-1} near the surface to 0.0041 kg kg^{-1} at 175 cm, while their median ρ_b remains close to 1.55 g cm^{-3} across the selected depths. These conditions result in small median f_{vom} values, decreasing from 3.45% near the surface to 1.43% at 175 cm. In DE25c, affected grid points occur only from 50 cm downward, with median f_{moc} values between 0.0027 and 0.0042 kg kg^{-1}, median ρ_b values between 1.69 and 1.73 g cm^{-3}, and median f_{vom} values between 1.09 and 1.59%. These diagnostics confirm that the safeguard is activated in dense, low-SOC, mineral-dominated soils, where the

volumetric organic fraction remains small. Its effect on the effective bulk properties is therefore limited at the global scale. The larger f_{vom} values obtained in DE25c relative to DE25 should consequently not be interpreted as the result of a stronger activation of the safeguard. They mainly arise from the mineral soil compactness adjustment itself. Increasing $\rho_{bms}{}^{c}$ modifies the mixture inversion, shifts the diagnosed ρ_{bom} downward, and increases the inferred f_{vom} for a given (f_{moc},ρ_b) pair. This mechanism is independent of the numerical safeguard and explains why DE25c can show slightly larger f_{vom} than DE25 while activating the safeguard much less frequently.

Change made: We revised Sect. 2.2.2 to describe $f_{mom}{}^{*}$ as the regularized value of f_{mom} introduced as a numerical safeguard in the diagnostic computation of ρ_{bom}. We also revised Sect. 3.1.3 to quantify the occurrence of this safeguard, to report the corresponding median f_{moc}, ρ_b, and f_{vom} values, and to clarify that the affected grid points correspond to dense, low-SOC, mineral-dominated soils. Finally, we added hatching to Supplementary Figures S4 and S5 to show where the safeguard is active.

Remark 2: The mineral compaction parameterization introduced in Section 2.2.3 is an important component of the proposed framework, but it appears to be formulated primarily as a function of soil texture, without explicitly considering the thermodynamic state of the soil. In practice, soil compaction processes may depend on temperature-dependent properties such as liquid water and ice content. Frozen soils, for instance, are generally less compressible than unfrozen soils, which could affect the expression for compacted bulk density, particularly the values of the empirical parameters involved. It would therefore be helpful if the authors could clarify the assumptions behind the current formulation, especially whether it is intended to represent long-term equilibrium conditions. A brief discussion of the potential implications of ignoring temperature- or phase-dependent effects would strengthen the physical interpretation of the scheme. If possible, even a qualitative sensitivity discussion of this simplification would be valuable for assessing its robustness across climate regimes.

Response: We agree that mechanical soil compaction can depend on water content, ice content, temperature, clay swelling, and external loading. However, this is not the process represented by the DE25c adjustment. DE25c does not simulate dynamic mechanical compaction during the land surface simulation. It applies a static adjustment to the dry bulk density of the mineral fraction before the simulation, in order to diagnose dry-reference mineral hydraulic and thermal parameters that are more consistent with the gridded bulk-density constraint. The purpose of this adjustment is to account for the compactness state implied by the input dry bulk density when using purely mineral pedotransfer functions, such as CO84. As shown in Part 1 of this study, the residual overestimation of saturated water content mainly occurs for low-SOM samples with observed porosities below about 0.4 $m^3\ m^{-3}$. This bias was attributed to the texture-based Cosby-SC mineral PTF, which rarely predicts mineral saturated water contents below 0.4 $m^3\ m^{-3}$, even for dense mineral soils (Decharme 2025). This provides the main motivation for the DE25c adjustment, which uses the gridded dry bulk-density constraint to shift the mineral reference porosity toward lower, more realistic values in dense mineral-dominated soils. We therefore clarified in the Methods that DE25c represents a dry-reference mineral compactness adjustment, not a dynamic mechanical compaction scheme. The adjustment is used only to diagnose dry-reference mineral properties before the prognostic simulation. During the simulation, ISBA still computes the time-varying soil water, ice, and thermal states from these diagnosed parameters.

Change made: We revised Sect. 2.2.3 to clarify that the DE25c adjustment does not simulate dynamic mechanical compaction, but uses the gridded dry bulk density as a static compactness constraint on the mineral reference state. We also added that the companion paper showed that the texture-based Cosby-SC mineral PTF rarely predicts mineral saturated water contents below about 0.4 $m^3\ m^{-3}$, which motivates the compactness adjustment in dense mineral soils.

Remark 3: In several parts of the manuscript, the model evaluation is done primarily against the CTL experiment, rather than against independent observations. While such relative comparisons are useful for isolating the effects of the proposed parameterization changes, they do not necessarily tell us whether the

modified configurations are more realistic. Including observational or reanalysis-based benchmarks would therefore strengthen the manuscript. For example, in Figure 5, comparing total water content against observational datasets would help assess whether the simulated changes are genuine improvements. In Figure 10, where clear differences in soil temperature over the northern high latitudes appear between DE25 and DE25c, incorporating observed data would help determine which configuration performs more realistically. Also, the interpretation of standard deviation in Figures 5, 9, and 10 is not entirely clear, as reduced variability does not necessarily imply improved performance. Clarifying the diagnostic purpose would be helpful.

Response: We agree that differences relative to CTL should not be interpreted as observation-based performance metrics. This is also how they are used in the manuscript. The CTL-based diagnostics are not used to evaluate model performance, but as mechanistic diagnostics to isolate the hydrothermal response of the model to the different SOM parameterizations under the same atmospheric forcing, soil input data, vegetation distribution, and model configuration. This is the purpose of Figures 5 and 10: they show the internal sensitivity of the simulated soil water and soil temperature fields to the new parameterizations, not their agreement with observations. The observational evaluation is provided separately, using variables for which large-scale independent constraints are available. These include GRACE ΔTWS, river discharge, evapotranspiration, near-surface soil temperature, active-layer thickness, and the comparison of SoilGrids bulk density with WoSIS. In particular, the thermal response over cold regions is not assessed only from Figure 10, because the manuscript also evaluates active-layer thickness, which provides an independent constraint on the simulated ground thermal regime in permafrost-affected regions. We therefore do not add an observational benchmark to Figure 5. Direct observations of total soil water content are not available at the continental to global scale with the vertical resolution, soil-depth coverage, temporal consistency, and spatial coverage required for comparison with the ISBA soil column. Existing gridded soil moisture products either mostly constrain the near-surface layer or rely on land surface models and data assimilation systems. Such products are therefore not necessarily more independent or more reliable than the simulations analyzed here for evaluating vertically resolved total soil water content. The soil water response is instead interpreted through process consistency and through available integrated constraints, especially GRACE ΔTWS, discharge, and evapotranspiration. Similarly, Figure 10 (now Figure 11 after figure renumbering, see RC1) is intended to diagnose the vertical and spatial structure of the soil thermal response to the SOM parameterizations. The observational thermal evaluation is provided separately through near-surface soil temperature and active-layer thickness. Adding a direct observational comparison to Figure 10 would require a global vertically resolved soil temperature benchmark with consistent depth coverage and temporal sampling, which is not available for this purpose. The reported σ values are descriptive spatial standard deviations of the plotted fields or of the differences relative to CTL. They are not used as uncertainty estimates or skill metrics, and no conclusion in the manuscript is based on interpreting a lower σ as an improvement.

Minor comments

Remark 1: L125-140: the sentences describing SoilGrids 2.0 and the Princeton Global Forcing dataset read more like a methods section. It might work better to move part of this description to Section 2 to improve the flow and readability. The remaining text could be trimmed into shorter, more focused sentences.

Response: We respectfully disagree that these sentences reduce the readability of the Introduction. They do not provide a detailed methodological description of the experimental setup, but only identify the two datasets that define the global simulation framework: SoilGrids 2.0 for soil inputs and PGF for meteorological forcing. This information is useful at this stage because it provides the general context of the simulations presented later in the manuscript. The sentences are also short and do not include excessive technical detail. The detailed processing of the SoilGrids variables, their vertical remapping onto the ISBA grid, and the full forcing setup are described later in the Methods section.

Remark 2: In Figure 4, the uncertainty ranges (e.g., red versus pink shading) overlap heavily, making it hard to tell the different configurations apart. Adjusting the color scheme would improve interpretability.

Response: We agree that the overlap between uncertainty envelopes in Figure 4 could make the visual distinction between configurations less direct. We revised the figure by increasing the contrast between the DE25 and DE25c configurations, using a brighter red for DE25 and a distinct yellow tone for DE25c. The data and percentile ranges are unchanged.

Change made: We revised Figure 4 to improve the readability of overlapping uncertainty envelopes by increasing the color contrast between DE25 and DE25c

Remark 3: L678-680: the manuscript attributes the soil cooling in Figure 10 to increased total water content (Figure 5) and reduced thermal conductivity (Supplementary Figures S13-S14). However, the vertical patterns in Figure 5 and Figure 10 do not seem fully consistent. In Figure 5, DE16 shows increasing soil water content with depth relative to CTL, while DE25 and DE25c show differences that decrease with depth. In contrast, Figure 10 indicates that all configurations (DE16, DE25, DE25c) become increasingly colder with depth relative to CTL, a pattern more consistent with the reduced thermal conductivity shown in the supplementary figures S13-S14. It would therefore be helpful if the authors could clarify how soil moisture and thermal conductivity work together to produce the simulated vertical temperature structure.

Response: We agree that the vertical soil temperature response should not be interpreted as a direct mirror of the vertical changes in w_{gtot}. We revised this interpretation to clarify the respective roles of soil water and thermal conductivity. The increase in w_{gtot} modifies heat storage through the volumetric heat capacity and also affects the moisture-dependent component of λ_{soil}. However, the widespread decrease in soil thermal conductivity induced by mineral-organic mixing, shown in Supplementary Figures S13 and S14, provides the more direct mechanism limiting vertical heat transfer within the soil column. The colder subsurface response in Figure 10 (now Figure 11 after figure renumbering, see RC1) is therefore interpreted as the result of coupled changes in heat storage and heat transfer, not as a direct consequence of the vertical pattern of w_{gtot} alone.

Change made: We revised the interpretation of Figure 10 (now Figure 11) to clarify that the vertical temperature response results from coupled changes in heat storage and heat transfer. The text now distinguishes the role of increased w_{gtot} from the more direct role of reduced soil thermal conductivity in limiting vertical heat transfer.

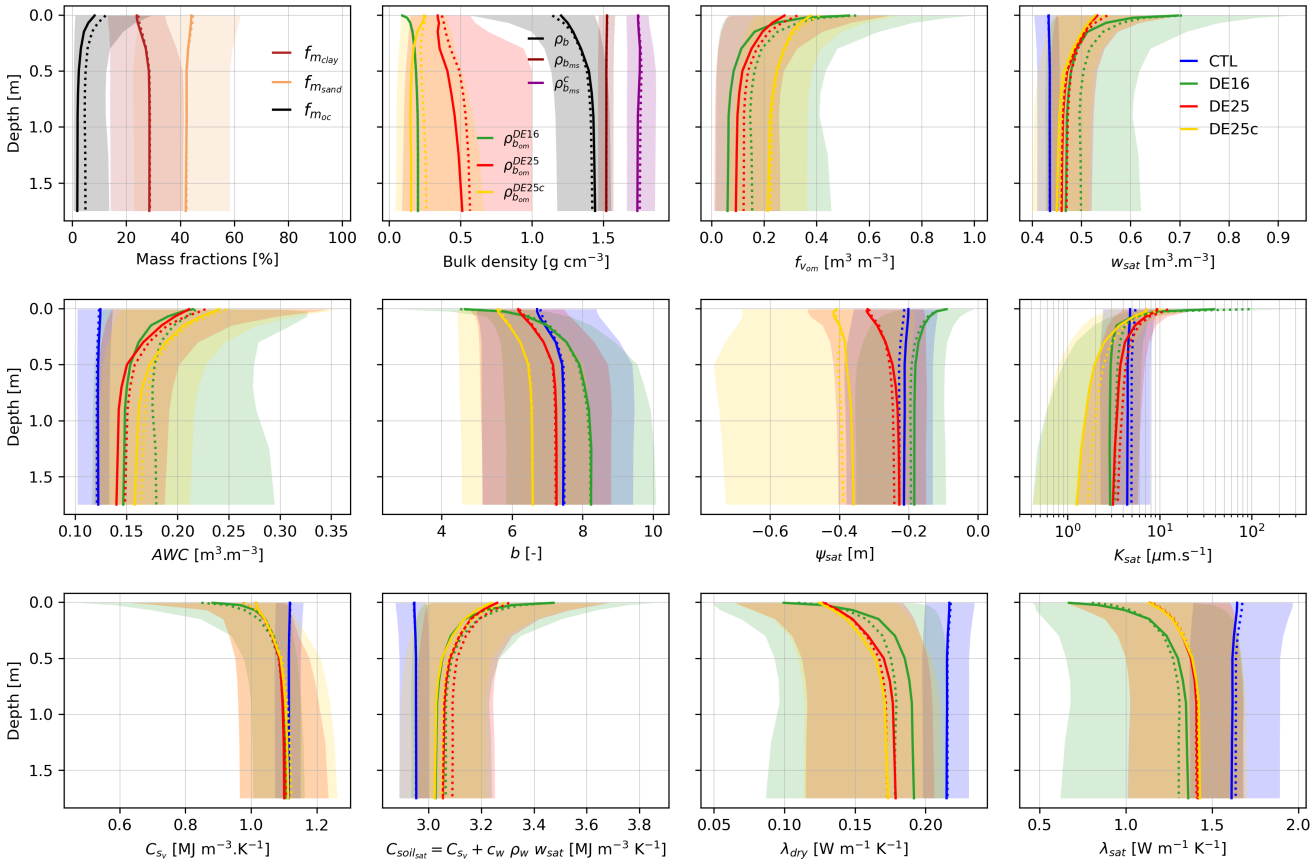

Figure 4. Global distributions of vertical profiles over the upper 2 m of the ISBA soil column, showing SoilGrids parameters ($f_{m_{clay}}$, $f_{m_{sand}}$, $f_{m_{oc}}$, and ρ_b), the derived phase-specific bulk densities ($\rho_{b_{ms}}$, $\rho^c_{b_{ms}}$, and $\rho_{b_{om}}$), and hydrological and thermal variables diagnosed in CTL, DE16, DE25, and DE25c. At each depth (positive downward), shaded envelopes indicate the 10th to 90th percentiles across land grid cells, solid lines show the median, and dashed lines show the mean. Variable definitions are provided in Figure 3 and Table B1.

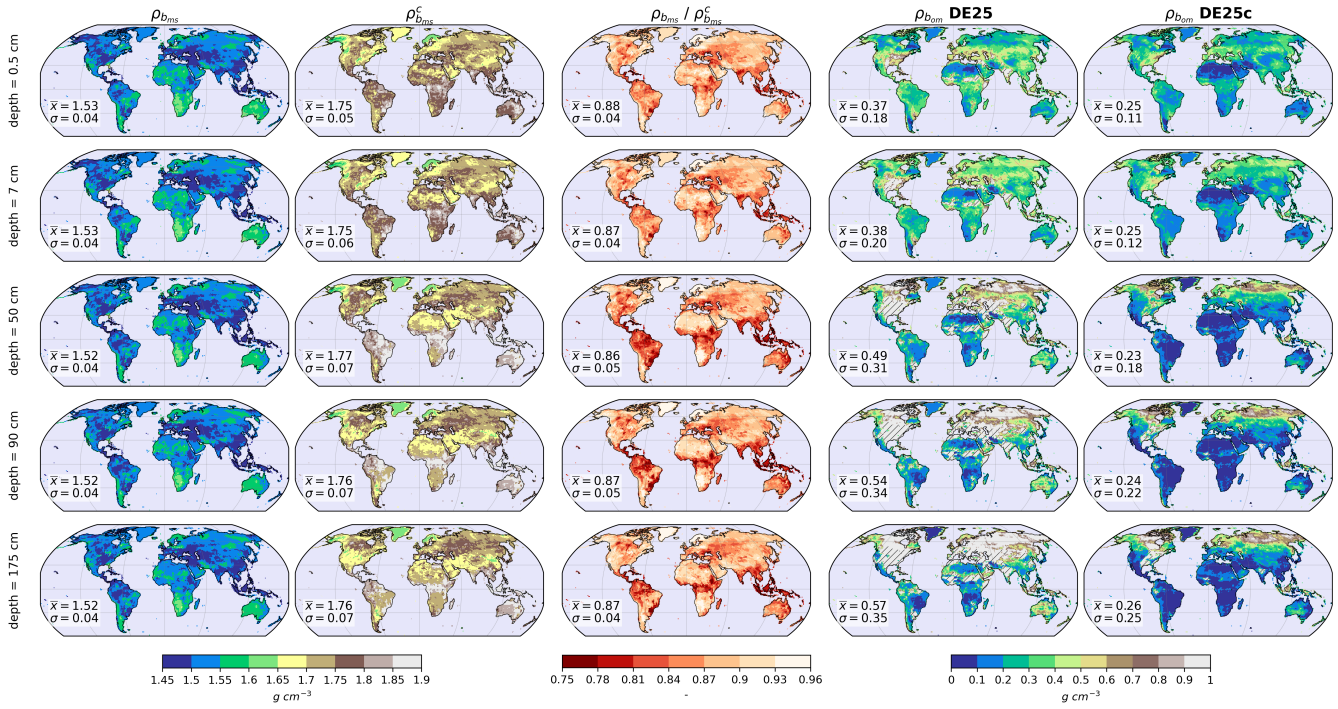

Figure S4. Global distributions of the mineral-phase bulk density $\rho_{b_{ms}}$ diagnosed in DE25, the compacted mineral-phase bulk density $\rho^c_{b_{ms}}$ diagnosed in DE25c, and their ratio $\rho_{b_{ms}}/\rho^c_{b_{ms}}$ (dimensionless), together with the diagnosed organic-phase bulk density $\rho_{b_{om}}$ for DE25 and DE25c, following the same layout and annotations as Supplementary Figure S3. Bulk densities are expressed in g cm^{-3}. Hatched areas in the $\rho_{b_{om}}$ panels indicate grid cells where the numerical regularization is active, i.e., where $f^*_{m_{om}} > f_{m_{om}}$ in the computation of $\rho_{b_{om}}$ (Equations 2 and 3).

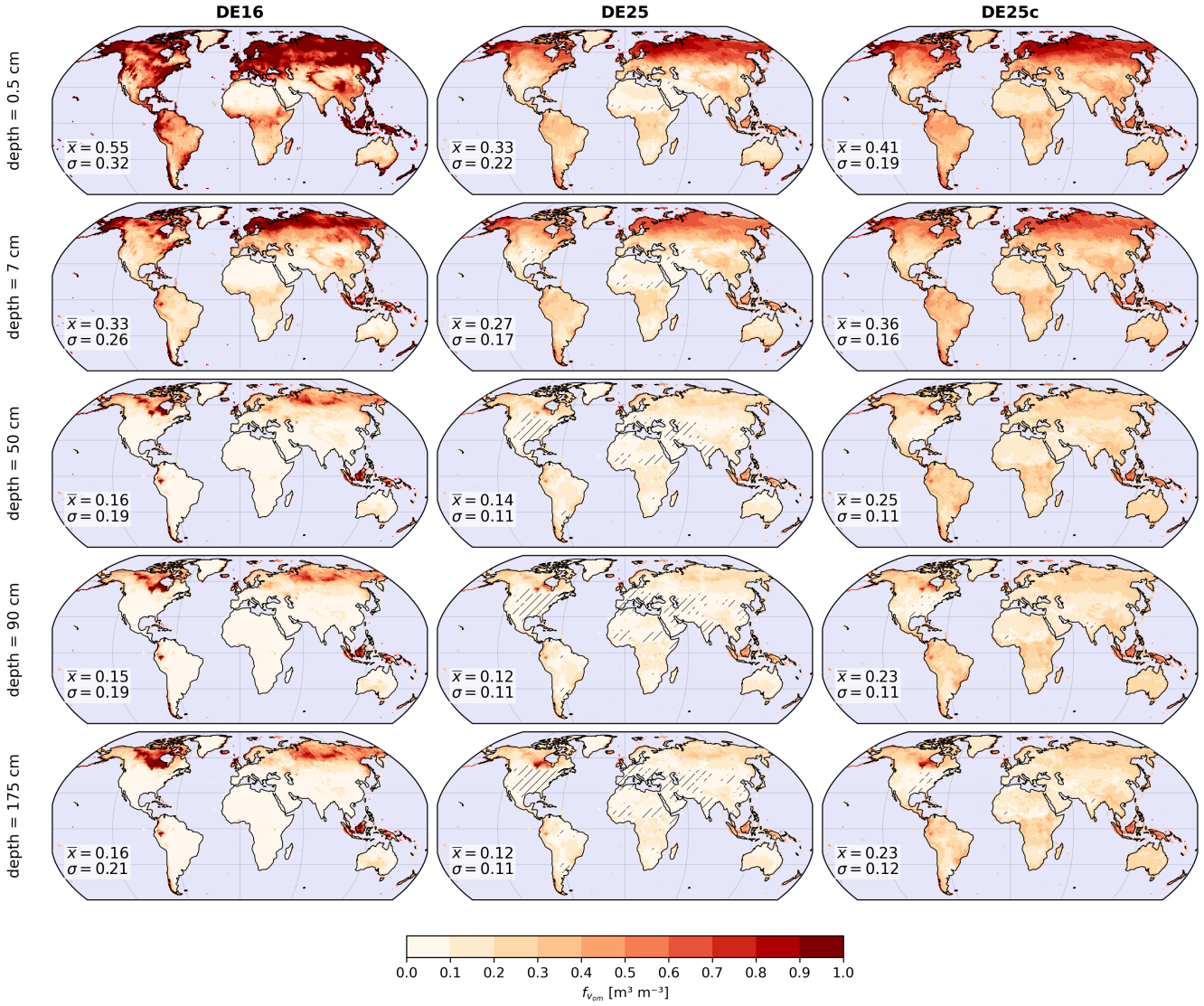

Figure S5. Global distributions of the volumetric organic matter fraction, $f_{v_{om}}$ (m^3,m^{-3}), diagnosed on the ISBA grid for the three parameterizations considered here (columns: DE16, DE25, and DE25c), using the same layout and annotations as Supplementary Figure S3. Hatched areas in the DE25 and DE25c panels indicate grid cells where the numerical regularization $f^*_{m_{om}}$ is active as in Figure S4.